ASSESSING THE IMPACT OF INTERANNUAL CLIMATE VARIABILITY ON NEW YORK CITY'S RESERVOIR SYSTEM

A Thesis

Presented to the Faculty of the Graduate School

Of Cornell University

in Partial Fulfillment of the Requirements for the Degree of

Master of Science

by

Mary Elizabeth Riley

May 2006

ABSTRACT

New York City's reservoir system supplies about nine million residents with approximately 1.3 billion gallons of water each day. Such dependence on the system requires a thorough understanding of the natural controls of its variability, as well as that of regional streamflow and precipitation. Prior studies suggest that climate variability in the Northeast depends upon large-scale northern hemisphere atmospheric and oceanic circulation patterns. In this study, the impact of large-scale climate variability on New York's reservoir system and whether interdecadal climate variations alter the influence of shorter interannual climate modes on water availability is examined. Also of importance is the interaction between these atmospheric oscillations and how these relationships might change during the different climatic regimes. Explored in this study are the influences of the Pacific Decadal Oscillation (PDO), El Niño-Southern Oscillation (ENSO), Pacific-North American Oscillation (PNA), North Atlantic Oscillation (NAO), and Atlantic Multidecadal Oscillation (AMO) on precipitation and hydrology in New York City's watershed. The direct impact of the large-scale oscillations on the quantity of water in New York's seven-reservoir system is also investigated. Statistical analysis has been performed on the data for 1951-2004, during which all data sets were available and, separately, for positive and negative PDO phases (1977-97 and 1951-76/1998-2004, respectively). The interactions between hydrological/meteorological factors and the reservoir system levels in the separate phases have also been

examined. Statistically significant differences in most interactions have been found between the separate PDO phases. The results of this study indicate that the potential for predicting reservoir behavior exists. Although statistically significant, the relationships are not well enough understood to prescribe using this information for watershed management at this point. However, the study results do warrant further exploration of the relationships between atmospheric/ oceanic oscillations and the reservoir system for practical watershed management applications.

BIOGRAPHICAL SKETCH

Mary E. Riley was born in Wilmington, Delaware and grew up in Sterling, Illinois. Desperate to leave the Midwest, she moved to Albuquerque, New Mexico and worked for several years prior to returning to school. She completed a BS in Earth and Planetary Sciences in 2002 at the University of New Mexico and returned to the world of minimum wage work briefly before entering graduate school at Cornell University for Atmospheric Science. Ms. Riley currently resides in Somerville, MA and is an environmental consultant for ICF Consulting in Lexington, MA. She is the semi-proud parent of two loud and needy cats.

ACKNOWLEDGEMENTS

The author would like to thank her advisor, Art DeGaetano, as well as her M.S. thesis committee members, Dan Wilks and David Pimentel. In addition, the author would like to thank the department of Earth and Atmospheric Sciences at Cornell University, the Northeast Regional Climate Center, the 11th floor graduate students, and Melissa Pfeffer of the Max Planck Institute of Meteorology for the contribution of support and resources.

TABLE OF CONTENTS

LIST OF TABLES

LIST OF FIGURES

INTRODUCTION

New York City's reservoir system supplies about nine million residents with approximately 1.3 billion gallons of water each day (Platt, et al. 2000). Such dependence on the system requires a thorough understanding of the natural controls of its variability, as well as that of regional streamflow and precipitation. Prior studies suggest that climate variability in the Northeast depends upon large-scale northern hemisphere atmospheric and oceanic circulation patterns. Specifically of interest to this study is the impact of large-scale climate variability on New York's reservoir system and whether interdecadal climate variations (i.e., regimes) alter the influence of shorter interannual climate modes on water availability. Also of importance is the interaction between these atmospheric oscillations and how these relationships might change during the different climatic regimes.

Arguably the most significant climate index for the United States as a whole is El Niño-Southern Oscillation (ENSO) (Gershunov and Barnett, 1998; Kahya and Dracup, 1993; Dracup and Kahya, 1994; Wang and Fu, 2000; Dettinger, et al., 2000; Rajagopalan, et al., 2000). While much research has been devoted to understanding how ENSO impacts individual regions, it has recently been suggested that the effects of ENSO in a particular region may not be consistent. The impacts may be different during opposing regimes, either being accentuated or dampened (Dettinger, et al., 2000; Mantua and Hare, 2002; Bradbury, et al., 2003; McCabe, et al., 2004).

In North America, statistically significant ($p \leq 0.05$) correlations between annual peak streamflows and December-February (DJF) Southern Oscillation Index (SOI) exist. In the United States, these relationships (both positive and negative) appear near coastal boundaries, but are almost nonexistent in the mid-section of the country (Dettinger, et al., 2000). However, these relationships display two different modes of response. There is an interdecadal contrast in the correlations between ENSO/global SSTs and streamflow. During the 1920s-1950s correlation was almost nonexistent. However, in recent decades the correlations are quite significant. For example, in the 1979-1995 period, peak streamflows in the Pacific northwest and northeast regions of the United States are generally below normal during El Niño years and above normal during La Niña years. Streamflows in the southern United States respond in a distinctly opposing fashion (Dettinger, et al. 2000). Kahya and Dracup (1993) conclude that ENSO events impact streamflow through changes in evaporation, transpiration, infiltration, and storage. These intermediate processes preclude a clearly defined linear relationship between ENSO and streamflow. Cayan and Peterson (1989) suggest that winter streamflow anomalies could possibly be predicted two seasons in advance using summer and fall SOI and one season in advance using the autumn Pacific-North American Oscillation (PNA) at least in the western United States, but this was not explored for the eastern United States. Dracup and Kahya (1994) further explore the ENSO/streamflow relationship and find a significant relationship between La Niña occurrence and streamflow anomalies in the

Northeast. Six out of eight La Niña years during the 1948-1988 study period corresponded to above-normal streamflow and two of the four extremely wet (defined as the top quartile of streamflow distribution) years in the entire period of study occurred during La Niña years.

In the northeastern United States, Dettinger, et al. (2000) report that La Niña events are significantly related to wet winters and summers. To a much less significant extent, El Niño brings dry conditions in the region. These relationships show up in regional streamflow, as well (1925 to 1984). Due to ENSO's persistence and slow development, the SOI during the previous June-August (JJA) is also correlated with peak annual streamflow, which occurs in approximately April (Dettinger, et al. 2000). Bradbury, et al. (2003), using rotated principal component analysis (RPCA), confirmed that Atlantic coastal/marine cyclonic activity increases during El Niño events while continental cyclonic activity increases during La Niña events, explaining the link to higher precipitation and streamflow in the interior northeastern United States as a result of La Niña. In addition, Wang and Fu (2000) find that overall winter precipitation in the Northeast is below normal during El Niño years. December temperatures in the region are as much as 2°C above normal during this phase, while January temperatures are only ~0.2°-0.4°C above normal. They suggest, additionally, that United States precipitation and temperatures respond to El Niño in a manner consistent with PNA patterns. This would mean El Niño is analogous to a positive PNA pattern, which typically brings warmer, drier conditions to the Northeast.

Dettinger, et al. (2000) propose that ENSO displayed less variability (weaker anomalies) during the 1930s-1960s than during the first decades of the 1900s or the post-1970 period. When Southern Oscillation variability is weak, they suggest that the hydrological teleconnection in South and North America weakens and possibly fails. Additionally, during the 1950s and 1970s La Niñas were more common while during the 1980s-1990s El Niños occurred more frequently. Bradbury, et al. (2003) acknowledge a step-wise increase in their first RPC for cyclonic activity that coincides with the phase-change of the Pacific Decadal Oscillation (PDO), from negative to positive, in the late 1970s.

Other large-scale climate factors, such as the North Atlantic Oscillation (NAO), Atlantic Multidecadal Oscillation (AMO), PNA, and PDO, have also been shown to influence the precipitation patterns in the Northeast. These atmospheric circulation patterns are defined and discussed in Appendix A.

Hartley and Keables (1998) observe that high winter snowfalls in the Northeast are associated with a meridional atmospheric circulation pattern, indicated by a negative phase of the NAO and a negative 700 hPa height anomaly over the eastern United States. For example, the more zonal circulation pattern that dominated prior to the 1950s abruptly became more meridional, apparently resulting in more significant snowfalls in the 1950s-1960s. A transition back to more zonal flow led to reduced snowfall in the 1970s-1980s. This decreasing trend in snowfall through the 1980s coincides with a tendency for strong positive anomalies in NAO. In contrast to these

findings, Bradbury et al. (2003) found that NAO does *not* correlate significantly with the primary modes of Northeast cyclones or precipitation patterns.

Hartley and Keables (1998) point out that only 42% of Northeastern snow variance can be explained by temperature and precipitation alone. They found: dry winter conditions in the Northeast to be associated with a positive 700 hPa height anomaly over the midwestern and eastern United States, while wet conditions result from higher cyclonic activity over New England and the Great Lakes regions, as well as positive sea surface temperature anomalies (SSTAs) off the East Coast. Warm conditions seem to be related to an anomalous 700 hPa high over the Canadian Maritimes that restricts polar air from entering the northeastern United States and colder-than-normal conditions are related to an anomalous 700 hPa trough over New England with positive height anomalies to the west and negative SSTAs southeast of New England. Snowy winters occur more often in the negative NAO pattern with more blocking over Greenland and an active Atlantic coastal storm track (Hartley and Keables 1998).

Mantua and Hare (2002) propose that the phase of the PDO is a significant contributor to ENSO's impact on streamflow, precipitation, and temperature anomalies throughout most regions of the United States. While the impact of this relationship in eastern New York is unclear, Nigam, et al. (1999) link the PDO with drought and streamflow patterns in the northeastern US. This was particularly expressed during the 1960s drought period when large (warm) SST anomalies dominated the North Pacific. These anomalies provide the

"fuel" for upper tropospheric circulation anomalies over the drought area, opposing the inflow of low-level moisture over the eastern United States. Additionally, SSTAs in the Atlantic adjacent to the Northeastern drought area suggest a feedback between local SSTs and the circulation anomalies, contributing to persistence of the drought (Nigam, et al. 1999). McCabe, et al. (2004) found that 52% of spatial and temporal variance in the multidecadal drought frequency over the continental United States can be attributed to PDO and AMO, with an additional 22% of the variance related to an increase in Northern Hemisphere temperatures. In northeastern United States climate divisions, there is an overall negative correlation between PDO and drought frequency. Performing RPCA of 20-year moving drought frequencies for 344 climate divisions in the US produced three leading components. The first three principal components (PCs), with PC1 and PC2 correlated to PDO ~0.82 and to AMO ~0.91, respectively, explain 74% of drought variance. They also state that recent droughts (1996, 1999-2002) were associated with North Atlantic warming (+AMO) and Eastern/Tropical Pacific cooling (-PDO). Additionally, AMO appears to significantly impact winter patterns of rainfall variability over most of the continental United States associated with ENSO (Enfield, et al. 2001).

Suggesting significant linkages between Atlantic and Pacific atmospheric and oceanic circulation patterns, Schwing, et al. (2003) suggest that decadal fluctuations in the patterns associated with each ocean have similar change points and are teleconnected, but with multiple modes. The PDO changes phase around 1924, 1947, and

1977 (with minor fluctuations in 1942, 1961, and 1987) (Appendix A); NAO's dominant mode transitions approximately at these points, as well (Appendix A). PDO's phase changes are most significant in 15-25 year and 50-70 year intervals, with only minor fluctuations more frequently (Mantua and Hare 2002). The regime duration for NAO varies from 5-37 years and is 16 years on average. Decadal changes in PDO and NAO were negatively correlated (out of phase) prior to the late 1950s, but positively correlated (in phase) during 1962-1988. It is also suggested that the strong El Niño event of 1957-58 contributed to the mode shift (Schwing, et al. 2003).

In this study a diagnostic approach is taken to examine the influence of these atmospheric circulation patterns on hydrologic variables in the New York City watershed. Within the watershed, streamflow, precipitation, snowfall, and reservoir levels are examined for evidence of a relationship to hemispheric climate patterns. Initially the relationships between the circulation indices and the hydrologic variables were examined individually. However, given the previous national studies these relationships were also examined conditional upon the phase of the PDO. Previous works, while suggesting that PDO phase exerts an influence on ENSO and NAO teleconnections, have not quantified the statistical significance of the apparent change. Such an analysis is conducted in this study. The potential of extending the diagnostic results to seasonal predictions of water resources impacts in the Northeast is also explored.

DATA

The climatological and hydrological data for this study have been obtained as follows. Reservoir level information (total %-of-capacity [%C]) was obtained for the Neversink, Pepacton, Cannonsville, Rondout, Ashokan, Schoharie, and Croton reservoirs, all of which are located in southeastern New York state (Fig. 1).

Figure 1: New York City's Reservoir System (Image courtesy of http://www.catskillcenter.org/programs/csp/H20/Lesson4/nycmap.gif)

This information was acquired for the 1st of each month from two sources, the New York Department of Environmental Protection (NYDEP) for 1947-1995 and the remainder (1996-2004) from NYDEP data published in the New York Times. This date, the 1st of each month, was arbitrarily chosen to ensure consistency of the information. Reservoir levels expressed as %C minimized the impact of manual manipulation of individual reservoirs resulting from management practices, such as systematic water releases and also partially mitigated changes in system capacity that occurred over time.

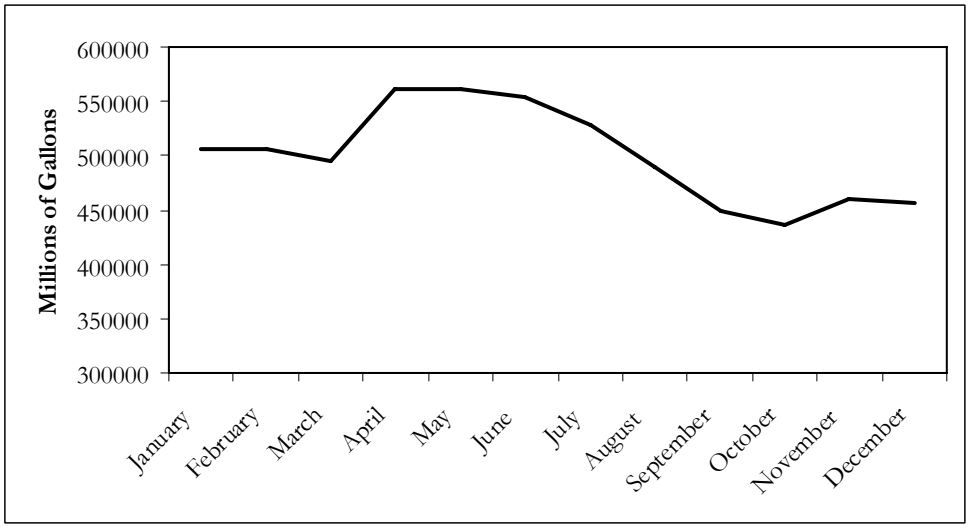

Figure 2: Annual Cycle, New York City Reservoirs

Reservoir levels are typically at a maximum in May and fall to a minimum in October (Fig. 2). Thus, conditions in winter and spring are important for reservoir recharge. In this study, %C on May 1 is used as a gauge for winter recharge. To account for the addition of the Cannonsville reservoir in 1965, which increased the total capacity of the system to 547.5 billion gallons, the reservoir levels were normalized (Fig. 3b), using the mean and standard deviation specific to

the pre- and post- 1965 periods (Fig. 3). This change had little effect on the nature of the overall %C time series, which is plotted for 1947-2004 (Fig. 3a, b). Because the data were heavily skewed to the right, it was preferred to transform the data into a more normal distribution. From the initial standardized values, the lowest value was added to all data points to make all data positive. After dividing all points by the highest value, it was possible to fit the series to a beta distribution (all values between 0 and 1). From this distribution's cumulative density function (CDF), also known as the incomplete beta function, z-values were found (Wilks, 1995). This series provided the normally-distributed values needed for analysis.

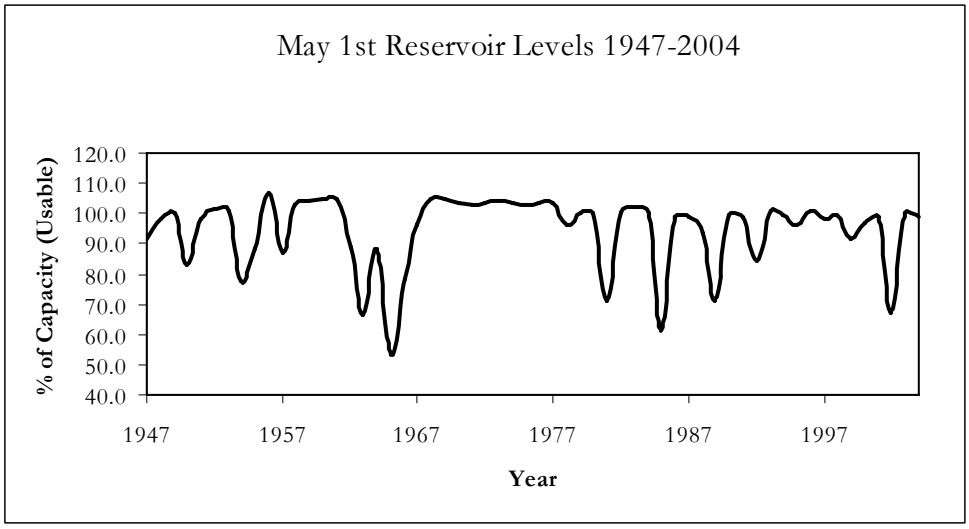

Figure 3a: Total Raw %-of-Capacity Reservoir System Levels

Although we have attempted to minimize the impact of management practices on the integrity of reservoir data, it is still almost certainly a factor. Water consumption trends also complicate the reservoir analysis. "Absolute" consumption was fairly consistent through the early 1960s and declined during the 1960s drought era. Per-capita

consumption steadily increased post-1966 through the mid-1980s (DeGaetano, 1999).

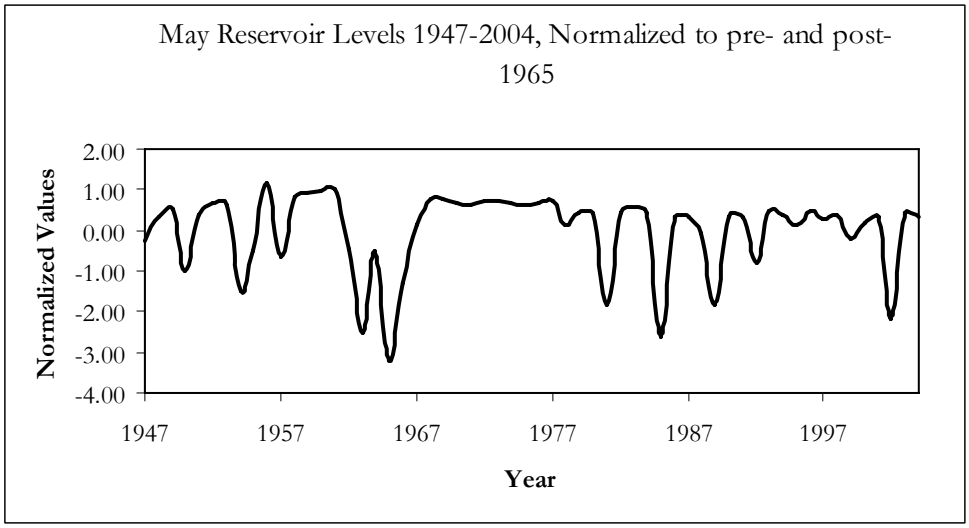

Figure 3b: Reservoir System Levels, Normalized

However, decreases in population during this period kept absolute consumption levels constant. After the mid-1980s, total consumption has remained steady even with positive population growth given decreased per-capita consumption (DeGaetano, 1999).

Since the reservoirs are within several climate divisions (Gutman and Quayle, 1996) that encompass a wider geographical area that is not likely representative of precipitation within the watershed, the precipitation data used in the study have been obtained from a watershed-specific "climate division," utilizing precipitation gauge data only from within and around the perimeter of the reservoirs' watersheds (Figure 4). In this new division, 30 rain gauge locations, some with records available for 1948-2004, and some with only partial records, were employed. The average precipitation for all available stations in a given month was used, as is standard procedure for the

traditional climate division meteorological data. The precipitation data were obtained from the Northeast Regional Climate Center (NRCC). During any given month within the study period, there were between 14 and 22 stations providing data (Figure 5).

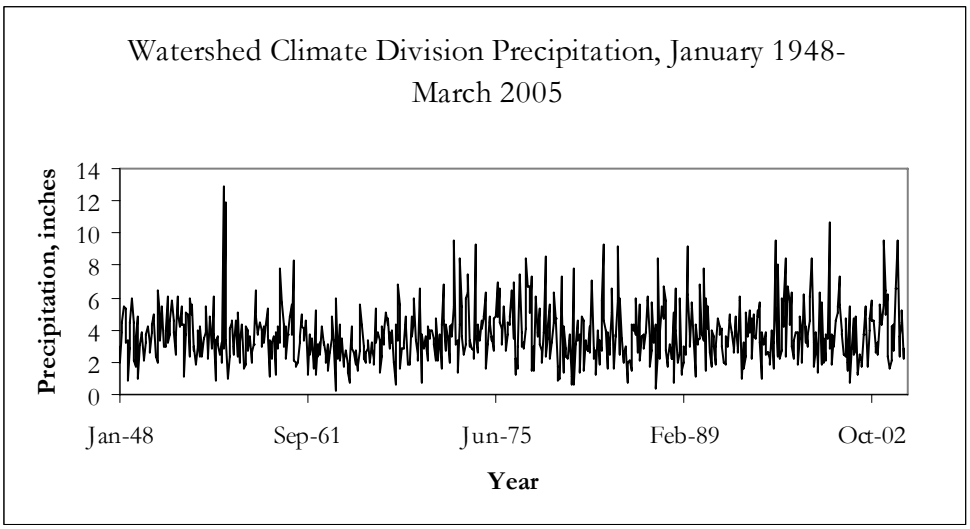

Figure 4: Watershed division precipitation

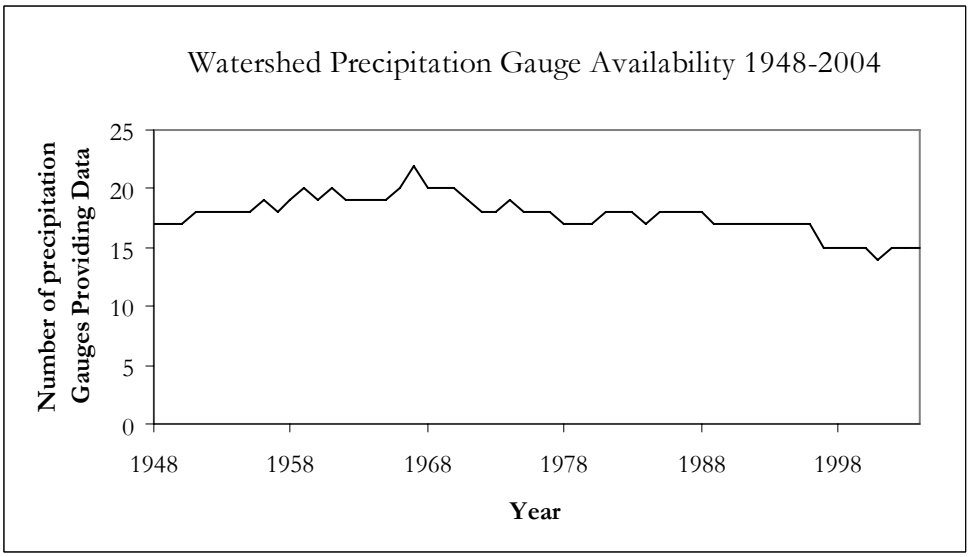

Figure 5: Number of Precipitation Gauges Reporting Data

The average location of the available stations varied only slightly with time, latitude fluctuating between 41.85° and 42.03° North, longitude

between 74.32° and 74.47° West, and elevation from 974 ft above sea level to 1220 ft above sea level (Figure 6). Additionally, there is no significant precipitation trend with time (Fig. 4). Total monthly precipitation was utilized; the accumulated precipitation for the previous n (n = 1,...,12) months prior to the May reservoir peak was analyzed in order to determine the period most highly correlated to the reservoir level (Fig. 7).

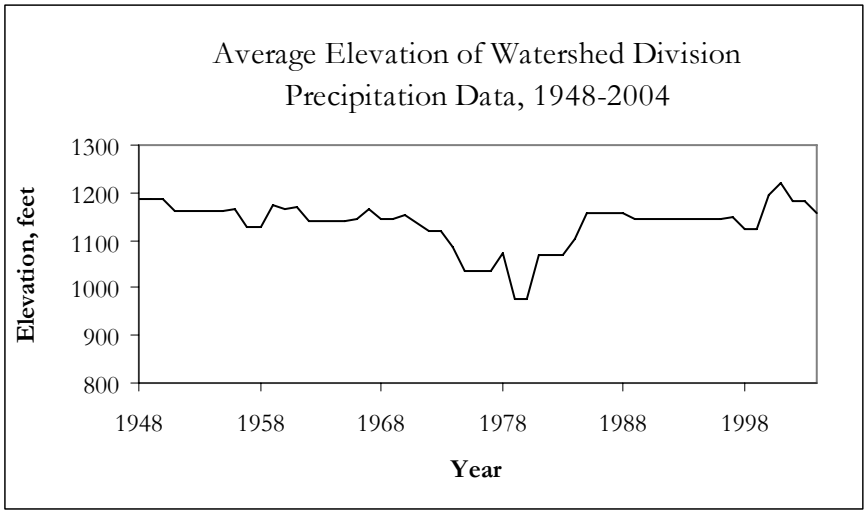

Figure 6: Average Elevation of Precipitation Gauges

Also, average snowfall and maximum snow depth (Table 2) data were computed for the watershed division. The availability of these data is much sparser than for total precipitation. Reliable snowfall information was available at a total of 22 stations within the division and, at any one time, between three and thirteen stations provided snow data (Fig. 8). The average latitude for the snow data stations varied between 41.77° and 42.21° North, longitude between 74.29° and 74.74° West, and elevation between 985 feet and 1470 feet above sea level (Fig. 9).

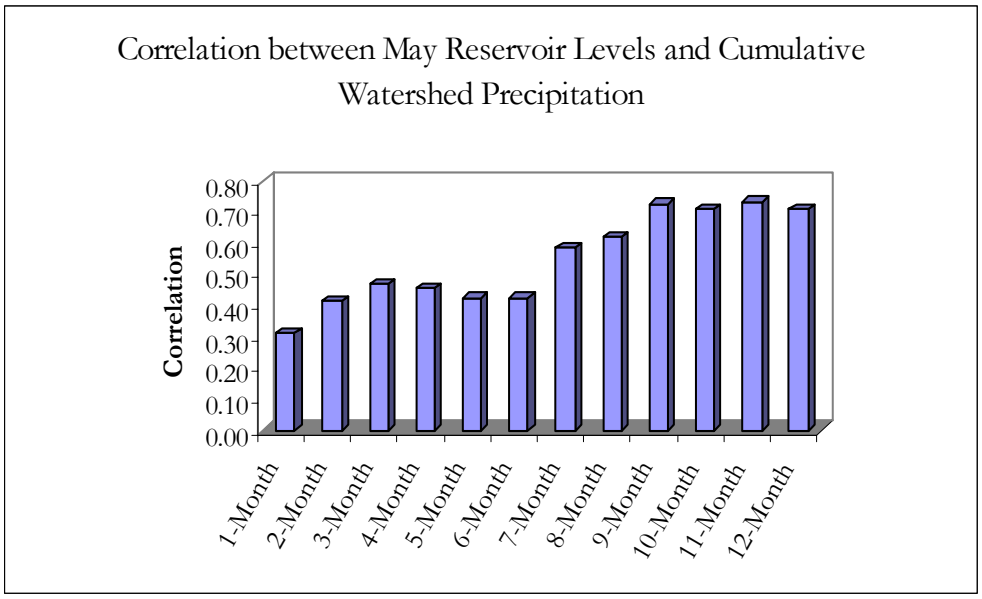

Figure 7: Correlations between Precipitation and May Reservoir Levels

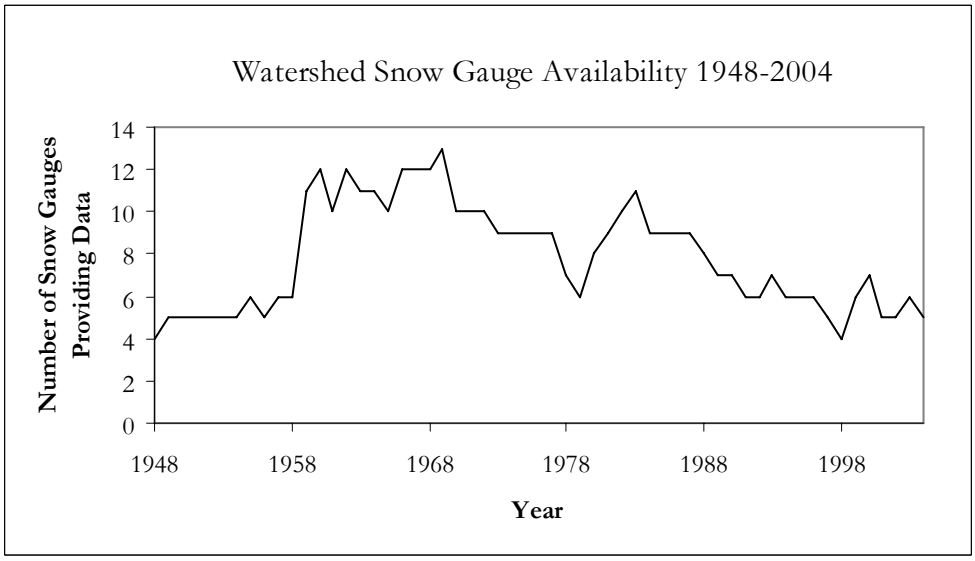

Figure 8: Number of Snow Gauges Reporting Data per Year

The United States Geological Survey (USGS) website, http://nwis.waterdata.usgs.gov/ny/nwis, provided monthly streamflow data. Gauge sites were chosen such that they comprise a major component of the reservoir system inflow, are minimally

influenced by human manipulation, and have the most complete period of record for the 1948-2004 period (Table 3). A total of ten sites were included in the monthly system average. For each site, monthly flow was taken as a percentage of the average monthly flow at that site. The data from the 10 gauges were averaged to create a system-wide percentage of average monthly flow.

Table 1 Watershed Precipitation Stations

Precipitation Gauge Location Name	Station ID	Latitude	Longitude	Elevation (ft)	Period of Record
Arena	300237	42.10	74.72	1450	1950-70
Arkville 2NW	300254	42.13	74.65	1310	1950-2004
Bedford Hills	300511	41.23	73.72	430	1950-77
Cairo 4NW	301095	42.32	74.03	490	1979-2004
Carmel	301207	41.43	73.68	530	1950-83, 2004
Carmel 4N	301211	41.47	73.66	680	2002-04
Claryville	301521	41.92	74.60	1653	1950-67, 81-04
Claryville 2SW	301523	41.92	74.60	2080	1967-78
Delhi 2SE	302036	42.25	74.90	1440	1950-71, 81-04
Downsville	302164	42.08	75.00	1112	1950-67
Downsville Dam	302169	42.08	74.97	1300	1959-88, 2000-04
East Jewett	302336	42.24	74.14	1991	1985-2004
Manorkill	305032	42.38	74.32	1620	1950-96
Merriman Dam	305276	41.80	74.43	865	1961-2003
Middletown 2	305312	41.43	74.42	502	1974-80
Middletown 2NW	305310	41.46	74.45	700	1951-2004
Neversink	305671	41.83	74.65	1302	1950-59
Phoenicia	306567	42.09	74.31	870	1950-2000
Pleasantville	306674	41.13	73.78	320	1950-99
Prattsville	306839	42.33	74.44	1207	1950-58, 66-97
Prattsville 2	306842	42.32	74.43	1142	1958-60
Shokan Brown	300985	41.95	74.20	510	1950-2004
Stamford	308160	42.40	74.63	1779	1950-2004
Tannersville 2E	308405	42.20	74.10	1923	1959-74
Walton	308936	42.17	75.13	1240	1956-96
Walton 2	308932	42.17	75.13	1480	1997-2004
Walton 5NE	308935	42.17	75.13	1801	1950-56
Windham 3E	309516	42.30	74.20	1680	1950-61, 70-04
Windham	309514	42.30	74.25	1503	1961-69
Yorktown Heights 1W	309670	41.27	73.80	670	1967-2004

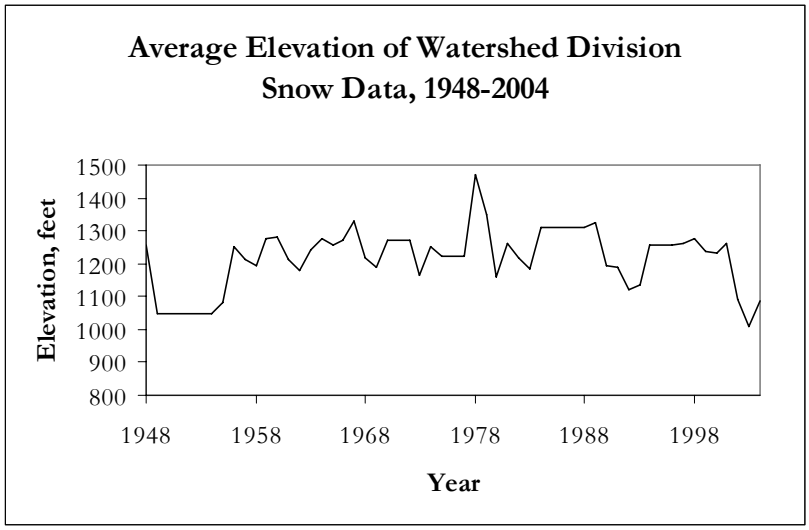

Figure 9: Average Elevation of Snow Gauge Sites

Table 2: Watershed Snow Gauge Stations

Snow Gauge Location Name	Station ID	Latitude	Longitude	Elevation (ft)	Period of Record
Arkville 2NW	300254	42.13	74.65	1310	1960-2004
Bedford Hills	300511	41.23	73.72	430	1950-55, 59-77
Carmel	301207	41.43	73.68	530	1950-77, 92-93, 2002-04
Carmel 4N	301211	41.47	73.66	680	2003-04
Claryville	301521	41.92	74.60	1653	1957-67, 81-2004
Claryville 2SW	301523	41.92	74.60	2080	1967-78
Delhi 2SE	302036	42.25	74.90	1440	1950-72, 81-2004
Downsville	302164	42.08	75.00	1112	1958-63, 65
Downsville Dam	302169	42.08	74.97	1300	1959-87
Middletown 2NW	305310	41.46	74.45	700	1951-55, 91-92, 95
Phoenicia	306567	42.09	74.31	870	1969, 80, 83, 90-91, 99-2000
Prattsville	306839	42.33	74.44	1207	1955, 57, 66-72, 74-88, 93-97, 2000-01
Prattsville 2	306842	42.32	74.43	1142	1959
Shokan Brown	300985	41.95	74.20	510	1962, 68-69, 73, 80, 82-83
Stamford	308160	42.40	74.63	1779	1981-90
Tannersville 2E	308405	42.20	74.10	1923	1959-74
Walton	308936	42.17	75.13	1240	1956-96
Walton 2	308932	42.17	75.13	1480	1999-2000, 2004-05
Walton 5NE	308935	42.17	75.13	1801	1948-56
Windham 3E	309516	42.30	74.20	1680	1959-60, 75-89
Windham	309514	42.30	74.25	1503	1962-67

The atmospheric-oceanic oscillation indices were obtained from multiple sources (see definitions in Appendix). The Pacific Decadal Oscillation (PDO) index chosen for this study was created by the Joint

Table 3: Streamflow Gauge Sites

Location	USGS ID	Yrs of Record
W. Branch Delaware at Walton	01423000	1950-2003
W. Branch Delaware at Hale Eddy	01426500	1950-2003
Trout Creek near Trout Creek	142400103	1952-67, 97-03
W. Branch Delaware upstream from Delh	01421900	1950-70, 97-03
Little Delaware River near Delhi	01422500	1950-70, 97-03
Tremper Kill near Andes	01415000	1950-2003
Neversink River near Claryville	01435000	1951-2003
Mill Brook near Dunraven	01414500	1950-2003
Schoharie Creek near Prattsville	01350000	1950-2003
Rondout Creek near Lowes Corners	01365000	1950-2003

Institute for the Study of Atmosphere and Ocean (JISAO) at the University of Washington and is updated at http://jisao.washington.edu/pdo/PDO.latest. JISAO uses "standardized values…derived as the leading principal component of monthly sea surface temperature anomalies (SSTAs) in the North Pacific Ocean, poleward of 20°N" with the global mean SSTAs removed.

The Pacific-North American (PNA) index is also produced by JISAO and is updated at http://www.jisao.washington.edu/datasets/pna/#digital_values. According to JISAO, this index was created using Wallace and Gutzler's (1981) formula, "PNA = 0.25 * [Z(20N,160W) - Z(45N,165W) + Z(55N,115W) - Z(30N,85W)], where Z is standardized 500 hPa geopotential height" at the specified location.

The normalized North Atlantic Oscillation index is produced by NOAA's Climate Prediction Center (CPC) and is calculated using RPCA. The 1950-2004 NAO data is available at http://www.cpc.ncep.noaa

.gov/products/precip/CWlink/pna/norm.nao.monthly.b5001.current.ascii.table.

Separate atmospheric and oceanic El Niño-Southern Oscillation (ENSO) indices were used. The oceanic component consists of area-averaged SST anomalies from the El Niño 3.4 (EN34) region. EN34 lies between latitude 5°N-5°S and longitude 120°W-170°W; this index, along with data from the other El Niño regions, is updated at ftp://ftpprd.ncep.noaa.gov/pub/cpc/wd52dg/data/indices/sstoi.indices. The atmospheric component of ENSO is the Southern Oscillation, a see-saw in effect, of high and low pressure systems between Papeete, Tahiti and Darwin, Australia. The Southern Oscillation Index (SOI) is the standardized Tahiti sea level pressure (SLP) - the standardized Darwin SLP (std Tahiti - std Darwin). The SOI was obtained from CPC, as well, and is housed at http://www.cpc.ncep.noaa.gov/data/indices/soi. The index is available here for 1951-present, and each monthly number is derived as a standardized anomaly from the averages recorded during 1951-1980.

The Atlantic Multidecadal Oscillation (AMO) index can be found at CPC's website, http://www.cdc.noaa.gov/Correlation/amo.us.long.data, and is available for 1871-2005. The area of interest in calculating the index is the entire Atlantic Ocean basin north of the equator. The index is presented as standardized anomalies of the 1951-2000 area-averaged SSTs.

METHODS

Statistical analyses focused on determining the relationships between the different hydrological variables and the atmospheric/ oceanic oscillations. The influence of these variables on the reservoir system was also assessed. A central focus was to determine if and how these statistical relationships change during different phases of the PDO (or PDO phase as a marker of hemispheric or global climate regime change), as suggested by the literature.

For each atmospheric/oceanic oscillation index (PDO, ENSO, PNA, NAO, AMO) 3-month averages were computed. Averages for Oct-Dec (OND) and Jan-Mar (JFM) characterized the reservoir recharge period. A Jul-Sep (JAS) average was also computed for the atmospheric indices to determine if this period provided predictive information. Average conditions over the entire Oct-Apr (O-A) recharge periods were also calculated. The autocorrelations for each data set (e.g. the correlation between the JFM average in year n and year n+1) were calculated to ensure that resampling tests would not need to be done in blocks. The degree of autocorrelation was also evaluated separately for years within the two PDO phases. The PDO is in its positive phase during the study years of 1977-97 and in its negative phase during the study years of 1951-76 and 1998-2004. However, the 1998-2004 period is less clearly defined, as it may just be a temporary negative 'blip' within the positive phase. This is still to be determined. It is noted that all tests involving precipitation, streamflow, and snow data have been limited to 1951-2003 because

this was the period for which all hydrological time series were available.

Additionally, correlations between each of the hydrological factors (using JAS, OND, and Oct-April, as well) for the positive PDO, negative PDO, and entire study periods were calculated. The interactions between the oscillations themselves were also explored, using correlations between each 3-month block of climate oscillation indices (for the year prior to the May reservoir level of interest).

Correlations between the oscillations and streamflow, snowfall, and precipitation were calculated as a comparison for intermediate processes (between atmospheric processes and reservoir levels). Initially, these correlations between the oscillations and the hydrological/meteorological indices were performed for the entire period that data was available for all indices, 1951-2003. Because information found in literature review suggests that the PDO phase alters the interactions between hydrological factors and large-scale oscillations, correlations between all data were also calculated separately for +PDO and –PDO time periods.

Correlations that differed by more than 0.4 (approximately the minimum significant correlation during the shortest period, positive PDO years) between PDO phase were evaluated using a Monte Carlo test to determine the probability that such a difference in correlation could occur randomly. Given the lack of significant autocorrelation in the time series of the atmospheric indices and hydrologic observations, 10,000 random series were generated by reassigning the paired (i.e., the index and hydrologic variable from the same years) values to

randomly selected years. The correlation between the values in these random series was computed based on the observed (non-shuffled) PDO series. This allowed a distribution of 10,000 random correlation differences (+PDO vs. –PDO) to be generated. This distribution enabled the probability of the observed (non-randomized) correlation difference to be quantified. The computer code (written in Python) for this resampling procedure is given in Appendix B. The Monte Carlo testing was the final step in the diagnostic examination. Examination of predictive ability has been considered in the "Applications" section and will not be discussed with the diagnostic results.

RESULTS

Prior to calculating correlations between May reservoir levels/ hydrological factors (precipitation, snowfall, streamflow) and the atmospheric/ oceanic oscillation indices, autocorrelations for all oscillations in the periods of interest were calculated (Table 4). Based on a t-test with N-3 degrees of freedom (N is the number of years in the time series), only the AMO had statistically significant ($p \leq 0.05$) autocorrelations. During negative PDO years and for the entire period of study significant auto-correlations for AMO JAS, O-A, and JFM existed at 1, 2, and 3 year lags (Table 4). During the positive PDO years, however, there are no significant autocorrelations for any of the indices. It is noted that 1977-1997 are marked as positive PDO phase, with 1951-1976 and 1998-2004 considered negative PDO phase.

Table 4: Atmospheric/Oceanic Oscillation Indices Autocorrelations

All Years				**Negative PDO**				**Positive PDO**			
Index	Lag-1	Lag-2	Lag-3	Index	Lag-1	Lag-2	Lag-3	Index	Lag-1	Lag-2	Lag-3
PDO O-A	0.356	0.249	0.167	PDO O-A	0.158	0.022	0.067	PDO O-A	0.16	-0.005	-0.106
PDO JAS	0.274	0.193	0.126	PDO JAS	0.173	0.121	0.258	PDO JAS	0.213	-0.002	-0.008
NAO JAS	0.112	0.234	0.274	NAO JAS	-0.29	0.363	0.367	NAO JAS	0.094	-0.1	-0.239
NAO O-A	0.252	0.255	0.199	NAO O-A	-0.02	0.134	0.118	NAO O-A	0.318	-0.162	-0.039
PNA JAS	-0.04	0.203	-0.06	PNA JAS	-0.12	0.168	0.011	PNA JAS	0.062	0.277	-0.083
PNA O-A	-0.03	-0.11	0.226	PNA O-A	-0.03	0.093	0.187	PNA O-A	0.233	0.488	-0.237
EN34 JAS	0.177	0.229	-0.029	EN34 JAS	-0.16	-0.174	0.032	EN34 JAS	0.247	0.378	-0.031
EN34 O-A	0.062	0.359	-0.076	EN34 O-A	-0.08	-0.339	0.003	EN34 O-A	0.086	0.462	-0.196
SOI JAS	-0.14	0.142	-0.124	SOI JAS	0.183	-0.003	0.096	SOI JAS	-0.19	0.398	-0.193
SOI O-A	-0.04	-0.089	-0.01	SOI O-A	-0.04	-0.175	-0.062	SOI O-A	-0.12	0.257	-0.062
AMO JAS	0.534	0.542	0.377	AMO JAS	0.616	0.693	0.573	AMO JAS	0.25	-0.099	-0.205
AMO O-A	0.718	0.626	0.518	AMO O-A	0.758	0.714	0.623	AMO O-A	0.439	-0.119	-0.171
PDO JFM	0.432	0.332	0.317	PDO JFM	0.244	0.202	0.263	PDO JFM	0.298	-0.039	-0.025
NAO JFM	0.33	0.312	0.317	NAO JFM	-0.17	0.251	0.341	NAO JFM	0.328	-0.172	-0.076
PNA JFM	-0.03	-0.027	0.218	PNA JFM	-0.03	0.206	0.244	PNA JFM	0.244	0.253	-0.133
EN34 JFM	-0.05	0.381	-0.069	EN34 JFM	-0.06	0.376	0	EN34 JFM	-0.076	0.456	-0.174
SOI JFM	-0.04	-0.093	-0.019	SOI JFM	-0.09	0.215	-0.062	SOI JFM	-0.161	-0.146	-0.089
AMO JFM	0.683	0.58	0.514	AMO JFM	0.722	0.673	0.59	AMO JFM	0.416	-0.063	-0.032

Additionally, the May reservoir levels' autocorrelations were not statistically significant for lags of 1, 2, and 3 years (r = 0.151, -0.145, and -0.022, respectively). The shaded cells in Table 4 indicate correlations greater than 0.5.

Table 5 summarizes the correlations between the atmospheric indices, both over the entire 1951-2004 period and within the different PDO phases. Correlations that are noticeably different in each period ($\geq$ 0.4 correlation differences) were chosen as candidates for further Monte Carlo tests.

In Table 5, the highlighted cells contain the correlation differences that are significant at the 5% level (i.e., less than 500 out of the 10,000 randomizations of those datasets met or exceeded the correlation differences, between positive PDO years and negative PDO years, seen in the table). For example, in Table 5 the correlation of the October-April PNA (PNA O-A) index average with the JFM-averaged Niño3.4 (EN34 JFM) index is 0.23 during negative PDO years, but is -0.50 during positive PDO years. During reshufflings of the time series' orders, correlations that are as different as 0.725 (0.23 - -0.50) only occurred 4 out of 10,000 times. Based on the resampling tests correlation difference $\geq$ 0.4 are significant at the 5% level.

In a second example, the October-April averaged Niño3.4 (EN34 O-A) correlation with the October-April averaged PDO (PDO O-A) is 0.657 during negative PDO years, but is only 0.187 during positive PDO years. For these series, a Monte Carlo test found that 253 out of 10,000 reshufflings met or exceeded this correlation difference of 0.47.

Table 5: Correlations between Atmospheric/Oceanic Oscillation Indices

All Years																		
Index	PDO O-A	PDO JAS	NAO JAS	NAO O-A	PNA JAS	PNA O-A	EN34 JAS	EN34 O-A	SOI JAS	SOI O-A	AMO JAS	AMO O-A	PDO JFM	NAO JFM	PNA JFM	EN34 JFM	SOI JFM	AMO JFM
PDO O-A	1																	
PDO JAS	0.361	1																
NAO JAS	0.018	0.107	1															
NAO O-A	0.04	0.362	0.172	1														
PNA JAS	0.145	-0.061	0.1	0.109	1													
PNA O-A	0.742	0.155	0.18	0.137	0.028	1												
EN34 JAS	0.534	0.56	0.19	0.039	0.093	0.633	1											
EN34 O-A	0.496	0.286	0.105	0.004	0.068	0.621	0.901	1										
SOI JAS	0.497	0.46	0.166	0.006	-0.04	0.614	-0.86	-0.82	1									
SOI O-A	0.562	0.377	0.054	0.135	0.052	-0.631	-0.78	-0.9	0.74	1								
AMO JAS	0.01	0.222	0.163	0.092	0.482	0.209	0.036	0.084	0	0.1	1							
AMO O-A	0.013	0.218	0.177	0.227	0.451	0.285	0.206	0.156	0.14	0	0.834	1						
PDO JFM	0.961	0.684	0.191	0.008	0.105	0.758	0.53	0.485	0.51	0.6	0.033	0.047	1					
NAO JFM	0.006	0.201	0.263	0.857	0.198	0.13	0.06	0.087	0.09	0	0.093	0.1	0.002	1				
PNA JFM	0.69	0.449	0.048	0.057	0.111	0.866	0.627	0.619	0.65	0.7	0.061	0.118	0.751	0.039	1			
EN34 JFM	0.451	0.427	0.027	0.019	0.056	0.598	0.851	0.986	-0.8	-0.9	0.107	0.141	0.434	0.081	0.588	1		
SOI JFM	0.552	0.5	0.098	0.113	0.069	0.662	-0.74	-0.88	0.7	1	0.104	0.054	0.531	0.03	0.7	-0.89	1	
AMO JFM	0.037	0.109	0.249	0.215	0.399	0.356	0.273	0.254	0.22	0.2	0.74	0.973	0.1	0.119	0.191	0.248	0.166	1

Table 5 (Continued)

Positive PDO Years																		
Index	PDO O-A	PDO JAS	NAO JAS	NAO O-A	PNA JAS	PNA O-A	EN34 JAS	EN34 O-A	SOI JAS	SOI O-A	AMO JAS	AMO O-A	PDO JFM	NAO JFM	PNA JFM	EN34 JFM	SOI JFM	AMO JFM
PDO O-A	1																	
PDO JAS	0.615	1																
NAO JAS	0.344	-0.063	1															
NAO O-A	0.192	0.332	0.316	1														
PNA JAS	0.431	0.032	-0.41	-0.039	1													
PNA O-A	0.663	0.089	-0.49	-0.073	0.271	1												
EN34 JAS	0.38	0.144	0.274	0.003	-0.06	-0.628	1											
EN34 O-A	0.187	0.357	0.013	0.192	-0.12	-0.519	0.811	1										
SOI JAS	-0.24	0.001	-0.246	0.006	0.042	0.571	0.848	0.789	1									
SOI O-A	0.234	0.382	-0.11	0.319	0.154	0.577	0.675	0.89	0.71	1								
AMO JAS	0.299	0.347	0.198	0.181	0.424	0.115	0.002	0.28	0.25	0.4	1							
AMO O-A	0.353	0.021	0.116	0.111	0.449	0.047	0.109	0.026	0.04	0.12	0.67	1						
PDO JFM	0.921	0.462	0.295	0.292	0.379	0.712	0.439	0.253	0.39	0.31	0.337	0.288	1					
NAO JFM	0.362	0.09	0.384	0.828	-0.15	-0.218	0.174	0.081	0.18	0.02	0.181	0.165	0.431	1				
PNA JFM	0.469	0.128	0.092	-0.051	0.351	0.845	0.633	0.577	0.68	0.7	0.308	0.111	0.634	-0.188	1			
EN34 JFM	0.159	0.042	0.2	0.254	-0.14	0.495	0.75	0.988	-0.73	-0.9	0.3	0.009	0.21	0.032	0.55	1		
SOI JFM	0.23	0.007	-0.352	-0.375	-0.18	0.556	-0.61	-0.83	0.66	0.98	0.373	-0.21	0.285	-0.109	0.688	-0.857	1	
AMO JFM	0.294	-0.16	0.297	-0.056	0.399	-0.181	-0.19	-0.2	-0.07	-0.1	0.488	0.93	-0.21	0.247	-0.07	-0.207	-0.03	1

Table 5 (Continued)

Negative PDO Years

Index	PDO O-A	PDO JAS	NAO JAS	NAO O-A	PNA JAS	PNA O-A	EN34 JAS	EN34 O-A	SOI JAS	SOI O-A	AMO JAS	AMO O-A	PDO JFM	NAO JFM	PNA JFM	EN34 JFM	SOI JFM	AMO JFM
PDO O-A	1																	
PDO JAS	0.71	1																
NAO JAS	0.356	0.539	1															
NAO O-A	-0.146	0.134	0.032	1														
PNA JAS	0.109	0.3	-0.312	0.262	1													
PNA O-A	-0.015	0.032	0.141	0.351	0.187	1												
EN34 JAS	0.639	0.074	-0.114	0.132	0.138	0.28	1											
EN34 O-A	0.657	0.164	0.183	0.22	0.073	0.23	0.95	1										
SOI JAS	-0.562	-0.057	-0.123	0.153	0.018	-0.148	-0.874	-0.828	1									
SOI O-A	-0.625	-0.121	-0.167	0.193	0.098	-0.15	-0.87	-0.933	0.732	1								
AMO JAS	0.246	0.054	0.271	0.033	0.5	0.436	0.079	0.035	0.167	0.05	1							
AMO O-A	0.403	0.057	0.171	0.151	0.437	0.558	0.313	0.306	0.35	0.31	0.054	1						
PDO JFM	0.959	0.614	0.357	0.137	0.167	0.014	0.609	0.608	0.519	0.56	0.343	0.494	1					
NAO JFM	-0.132	0.023	0.119	0.851	0.353	0.255	0.07	0.198	0.19	0.19	0.162	0.052	-0.083	1				
PNA JFM	0.789	0.516	0.079	0.297	0.159	0.006	0.647	0.644	0.603	0.58	0.374	0.461	0.804	-0.146	1			
EN34 JFM	0.603	0.695	0.2	0.247	0.043	0.23	0.91	0.984	-0.76	-0.9	0.013	0.296	0.551	0.224	0.606	1		
SOI JFM	-0.65	-0.709	0.13	0.256	0.074	0.116	-0.828	-0.916	0.7	0.96	0.091	0.341	0.583	0.217	0.655	-0.911	1	
AMO JFM	0.445	0.326	0.395	0.222	0.376	0.286	0.375	0.376	0.414	0.38	0.805	0.981	0.533	0.138	0.479	0.369	0.403	1

Comparing the results in Table 5 with information found in the literature suggests that many of the significant results in Table 5 have not been found elsewhere. Qualitatively, it has been recognized that the downstream impacts of ENSO are altered, depending on PDO phase (Dettinger, et al., 2000; Mantua and Hare, 2002; Bradbury, et al., 2003; McCabe, et al., 2004), a result confirmed by Table 5. As seen in Table 5, the O-A averaged PDO correlates quite strongly with EN34 O-A during negative PDO years, but not very well during positive PDO years. This is also true for the SOI. Quantitatively, there are no specifics found in the literature as to how the statistical relationship between ENSO and PDO is altered.

Wang and Fu (2000) found that ENSO does not modulate the PNA pattern. In this study, JAS EN34 and PNA were not found to correlate highly to each other in any period. However, JAS EN34 has been found to correlate highly ($r > 0.6$) to the following JFM PNA in all periods. Additionally, JFM EN34 displays a high *negative* correlation ($r = -0.5$) to PNA O-A during positive PDO years but only a moderate *positive* correlation to PNA O-A during negative PDO years ($r = 0.23$). During the entire period of study, the relationship is significantly positive ($r = 0.60$). Wang and Fu found a more significant relationship between North Pacific SSTs and PNA than between tropical Pacific SSTs and PNA. In Table 5, that is confirmed (using PDO for N. Pacific SSTs) during the overall period ($r = 0.74$ for the O-A period) and positive PDO years ($r = 0.66$ during O-A), but not during negative PDO years ($r = -0.02$). The summer PDO and PNA are not significantly correlated during these periods, though ($r = -0.06$ and $r = 0.03$).

However, during the negative PDO years, the PNA and PDO are significantly correlated during the summer (r = 0.3 during JAS). Schwing, et al. (2003) state that Atlantic and Pacific oscillations are correlated, but in multiple modes. For example, the oceans were "in phase" prior to 1957, but "out of phase" 1962-1988. They also suggest that the significant El Niño event of 1957-58 may have contributed to the shift, but do not provide any detail. However, this does not address the PDO phase as specifically impacting how the oscillations interact. Most other information found in literature review discusses how the oscillations interact with hydrological parameters, or how they may work together to affect hydrological parameters, but not how they correlate to each other.

Table 6 shows the correlations between the hydrological factors: precipitation, snowfall, and streamflow during OND, October-April, and JFM. Appropriate p-values for each sample size have been based on a simple chart of values calculated with a t-test with (N-2) degrees of freedom. For the entire study period, the correlations (r) are significant at the p = 0.05 level for $r \geq 0.226$ (52 degrees of freedom), for negative PDO years r is significant at p = 0.05 when $r \geq 0.291$ (33 degrees of freedom), and for positive PDO years, r is significant at the p = 0.05 level when $r \geq 0.369$ (21 degrees of freedom). It should be noted that these values weren't used for the threshold of significance for the autocorrelations in Table 4 because, with so few years, autocorrelations of less than 0.50 are not significant. Values that are noticeably different for each period are highlighted (Table 6). Cells containing "N/A" mark spaces where correlations between the two

variables are unnecessary, e.g., OND streamflow could not be a result of the subsequent JFM period's precipitation. The circled values are statistically significant. Some of the more significant results are expected, such as between OND precipitation and O-A precipitation due to OND being a subset of the longer period.

Table 6: Correlations between Hydrological Factors

All Years	May Res Level	JFM Precip	OND Precip	O-A Precip	JFM Snowfall	JFM Snow/ Precip Ratio	JFM Streamflow	OND Streamflow	O-A Stream-flow
May Res Level	1								
JFM Precip	.413	1							
OND Precip	.442	N/A	1						
O-A Precip	.656	.562	.782	1					
JFM Snowfall	.222	.165	N/A	.253	1				
JFM Snow/ Precip Ratio	.06	.877	N/A	.007	.877	1			
JFM Streamflow	.302	.694	.226	.525	.111	.371	1		
OND Streamflow	-.102	N/A	.052	.158	N/A	N/A	.289	1	
O-A Streamflow	.619	.482	.778	.821	.223	.017	.602	.202	1
Negative PDO Years	May Res Level	JFM Precip	OND Precip	O-A Precip	JFM Snowfall	JFM Snow/ Precip Ratio	JFM Streamflow	OND Streamflow	O-A Stream-flow
May Res Level	1								
JFM Precip	.331	1							
OND Precip	.501	N/A	1						
O-A Precip	.637	.488	.83	1					
JFM Snowfall	.136	.178	N/A	.084	1				
JFM Snow/ Precip Ratio	-0.01	.543	N/A	.257	.904	1			
JFM Streamflow	.269	.626	.212	.523	.473	.603	1		
OND Streamflow	-.137	N/A	.162	N/A	N/A	N/A	.18	1	
O-A Streamflow	.647	N/A	.77	.857	N/A	N/A	.594	.269	1

Table 6 (Continued)

Positive PDO Years	May Res Level	JFM Precip	OND Precip	O-A Precip	JFM Snowfall	JFM Snow/ Precip Ratio	JFM Streamflow	OND Streamflow	O-A Stream-flow
May Res Level	1								
JFM Precip	.645	1							
OND Precip	.334	N/A	1						
O-A Precip	.715	.693	.716	1					
JFM Snowfall	.372	.49	N/A	.566	1				
JFM Snow/ Precip Ratio	.173	.135	N/A	.333	.907	1			
JFM Streamflow	.41	.782	.295	.569	.238	.041	1		
OND Streamflow	.087	N/A	.067	N/A	N/A	N/A	.418	1	
O-A Streamflow	.592	N/A	.79	.777	N/A	N/A	.623	.117	1

There are results in Table 6 that are at least qualitatively significant. It is noted that the statistical relationship between the total JFM watershed precipitation and JFM snowfall is significant during positive PDO years, but is not significant during negative PDO years ($r = 0.49$ vs. $r = 0.178$) or during the entire study period ($r = 0.165$). It is also observed that streamflow is more persistent from OND to JFM during positive PDO years ($r = 0.418$) and over the entire study period ($r = 0.289$), but the persistence is not statistically significant during negative PDO years ($r = 0.18$). The other correlations in this table show little difference, or do not seem important to the study, in the different periods.

Of particular interest are the relationships between the oscillations and the hydrological factors or reservoir levels. Of the hydrologic variables analyzed in this study, October-April streamflow, JFM streamflow, October-April precipitation, JFM precipitation, JFM

snowfall, and May reservoir levels have significant correlation differences in different phases of the PDO with some of the oscillation indices (Table 7). The numbers in bold font are statistically significant at the p = 0.05 level, based on the aforementioned t-test with (N-2) degrees of freedom. Although many of the differences in the correlation between the periods exceed 0.4, the most significant difference in correlation between the different PDO phases (noted with

Table 7: Correlations between Atmospheric/Oceanic Oscillation Indices and Selected Hydrologic Variables

Correlations with JFM Snowfall			
Index	**All Years (1951-2003)**	**(+) PDO**	**(-) PDO**
NAO JFM	-.268	-.289	**-.35**
NAO JAS	-.129	**-.404**	.06
PDO JFM	.267	**.496**	.077
PDO O-A	.231	**.451**	.039
PDO JAS	.143	**.378**	-0.114
PNA JAS	-.347	**-.558**	-.14
Correlations with JFM Streamflow			
Index	**All Years (1951-2003)**	**(+) PDO**	**(-) PDO**
NAO JFM	.154	-0.271	**.504**
NAO OND	-.149	**-.498**	.077
NAO O-A	-.023	**-.562**	**.403**
PDO OND	-.086	-.299	.036
PNA JAS	.139	-.164	**.357**
AMO OND	.09	**.343**	-.041
Correlations with ONDJFMA Streamflow			
Index	**All Years (1951-2003)**	**(+) PDO**	**(-) PDO**
NAO JFM	.000	-.219	.146
NAO OND	-.12	**-.382**	.046
NAO O-A	-.104	**-.433**	.123
NAO JAS	.199	-.084	**.369**
AMO JFM	-.068	.233	-.203
AMO OND	.014	.293	-.112

Table 7 (Continued)

Correlations with May 1 Reservoir Levels			
Index	**All Years (1951-2003)**	**(+) PDO**	**(-) PDO**
NAO JAS	0.179	-0.012	**.264**
EN34 JAS	0	0.289	-0.055
SOI JAS	-0.047	0.292	-0.132
EN34 O-A	-0.054	**0.454**	-0.059
SOI O-A	-0.05	0.297	-0.134
PNA O-A	-0.063	-0.174	0.182
EN34 OND	-0.044	**0.431**	-0.056
SOI OND	-0.082	0.252	-0.141
EN JFM	-0.068	**0.44**	-0.04
Correlations with JFM precip			
Index	**All Years (1951-2003)**	**(+) PDO**	**(-) PDO**
NAO JFM	.119	-.16	**.311**
Correlations with ONDJFMA Precip			
Index	**All Years**	**(+) PDO**	**(-) PDO**
NAO JAS	.196	.051	**.264**
SOI OND	-.103	-0.229	.022
PDO JAS	.177	.241	.081
PNA O-A	**.247**	.2499	.217
PNA JAS	-.018	-.216	.15

an oval in Table 7) is between the NAO October-April average and the JFM average streamflow. During the positive PDO phase, the correlation is -0.562, indicative of a decrease in streamflow during the positive NAO phase (Fig. 10). Conversely, during the negative PDO years, the correlation is 0.403 (i.e., streamflow is enhanced during positive NAO years), as seen in Fig. 11. To confirm the significance of this difference, once again the Monte Carlo method has been employed. To ensure that the method could be run with reshufflings of single pieces of data, rather than in blocks, autocorrelations for the JFM streamflow at 1, 2, and 3 year lags have been calculated.

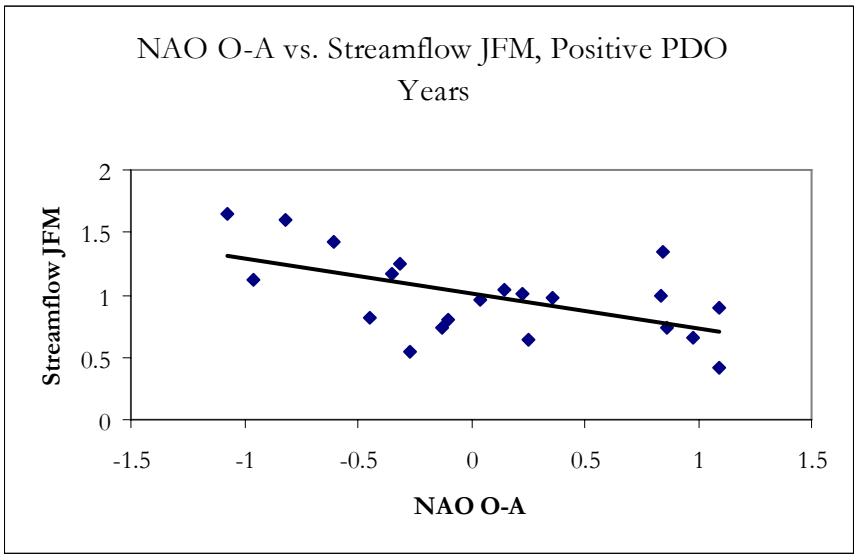

Figure 10: Scatterplot of NAO O-A and Streamflow JFM During Positive PDO Years; Trend Line Added.

At lags of 1, 2, and 3 years, the autocorrelations were 0.24, 0.31, and 0.20, respectively. Hence, no reshuffling in blocks was necessary. After 10,000 reshufflings of the series, a combination so significantly positive in negative PDO years and so significantly negative in positive PDO years occurred only three times.

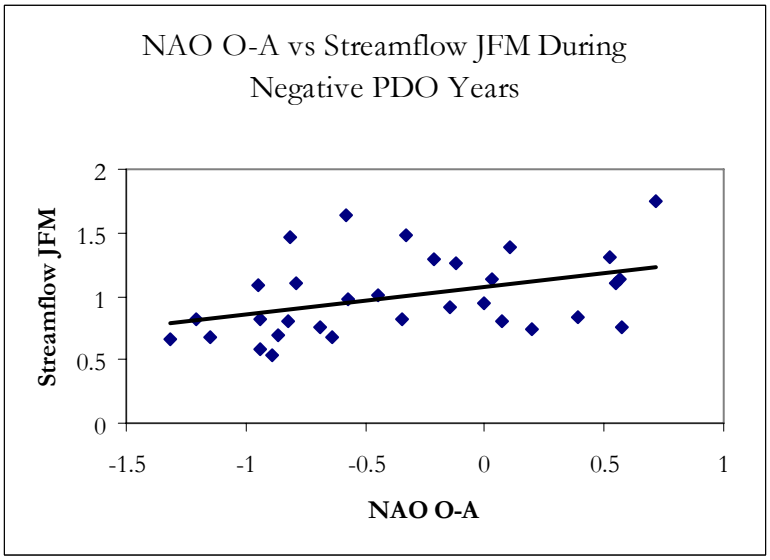

Figure 11: Scatterplot of NAO O-A and Streamflow JFM During Negative PDO Years; Trend Line Added.

Hartley and Keables (1998) found that from the late 1950s-60s, greater than average snowfall in the northeastern United States occurred with the predominantly negative NAO during that time. As seen in Table7, this study found that during the negative PDO years that characterized the 1950s and '60s JFM NAO has a significant negative correlation (r = -0.35) to snowfall in the NYC watershed, confirming Hartley and Keables' findings. During the other periods, there was still a negative correlation between the indices, but at non-significant levels. Here it is also found that the previous JAS NAO average negatively correlated with subsequent JFM snowfall in the watershed during positive PDO years, but not during the other periods. Hartley and Keables do not share a similar finding. Additionally, JAS and O-A PDO were highly positively correlated to JFM snowfall during positive PDO years, but not during the negative PDO phase. Another factor is the previous summer's PNA, which is highly negatively correlated to JFM snowfall during the negative PDO phase.

While Dracup and Kahya (1994) found a strong relationship between streamflow in the Northeast and ENSO, there was no evidence of this relationship in this study. However, ENSO is significantly correlated (r = 0.42) to May 1 reservoir levels during positive PDO years, but not during negative PDO years and for the study period as a whole. Similarly, Wang and Fu (2000) suggest that wintertime precipitation (here, O-A) responds to ENSO "in a way consistent with the PNA pattern." The results of this study suggest that this is not

true for the northeastern U.S., at least in a statistically significant manner. In fact, the only significant correlation between an oscillation and winter precipitation occurs between JFM precipitation and JFM NAO, and only during negative PDO years (0.31).

According to the results of this study that are displayed in Table 7, various periods of NAO and AMO are the only oscillations with any significant correlations to O-A streamflow. Dettinger, et al. (2000), however, found that seasonal SOIs are consistently correlated to streamflow in North America. In neither negative nor positive PDO years were any similar results for the NYC watershed found in this study. It is noted, though, that time series here were not broken up into La Niña and El Niño years, as the Dettinger, et al. study did. Additionally, Kahya and Dracup (1993) state that the relationship between ENSO events and streamflow is governed by intermediate processes (evaporation, transpiration, infiltration, and storage), which could explain the lack of a linear relationship in this study. They also found that, for their study years of 1948-88, the previous summer and fall PNA index "provide[s] guidance" for spring streamflow. This result is, in fact, confirmed here, but only during negative PDO years, during which the JAS PNA correlates positively with JFM streamflow (0.36). During the full study period, and also in positive PDO years, the correlation is not statistically significant.

This study has been primarily diagnostic. The results have been largely exploratory. The goal has been to seek out any statistically significant relationships that may exist between large-scale oscillations and the local hydrology, particularly those that vary with PDO phase.

To more fully understand the paradigm, more detailed studies into the mechanisms involved should be addressed. It would be useful in a practical sense to determine a diagnostic "formula" that works for each PDO phase, as it has been shown here that there is a discernible difference in the response of hydrological factors within New York City's watershed to climatic oscillations in the different phases of the PDO. If it is possible to understand the factors that influence annual peak reservoir levels, it may also be possible to then predict the availability of reservoir water. In this regard, the predictive capability of this knowledge is briefly introduced separately in the subsequent "Applications" section.

APPLICATIONS

This research has been primarily diagnostic in nature. Ideally, however, the most useful application of the study's results would be a method of prediction for the annual peak reservoir levels. In order to be able to predict May reservoir levels in New York City's watershed with any real value for resource planning, using information from the previous summer and fall is most practical (because these months represent the previous discharge-recharge period). To assess the system diagnostically, it is useful to examine the roles October-March oscillation indices in determining reservoir levels, as well as how these oscillations impact the intermediate hydrological factors: precipitation, snowfall, and total precipitation.

A brief exploration of the predictive capability of the oscillations for the different periods, with regard to annual peak reservoir levels and separately for each hydrological parameter, has been completed as a final step in this study. Lastly, the role of hydrological factors as predictors of the May reservoir levels has been examined.

The tests have been completed using linear discriminant analysis (LDA) and the results confirmed through cross validation (CV) (holding the best predictors found through LDA constant). Each analysis was run to determine the most accurate: 1.) single predictor, 2.) two predictors in combination, and 3.) three predictors in combination. These analyses were repeated for each period of interest: all years of the study, positive PDO years only, and negative PDO years only. Each time series used as a predictand was divided into two

groups, “above normal” and “below normal,” based on the mean of the full series. The skill for each run is given as a Kuiper skill score (KSS) (Wilks, 1995) and also how many correct predictions as above or below normal this corresponds to (i.e., x : n). The KSS equation is equal to {(ad – bc) / (a + c)(b + d)} where a is the number of predictions that were both forecast and observed, b the number of predictions that were forecast and not observed, c is the number that were not forecast but were observed, and d is the number of predictions that were not forecast or observed (Wilks, 1995). Also for each predictand in each time period, two sets of predictors were run separately. In one set were the O-A, OND, and JFM averages (diagnostic), and in the other the JAS averages (prognostic).

In attempting to classify JFM precipitation for the watershed division as above or below normal, the only combination of predictors that was useful in LDA occurred during the positive PDO period. Together, AMO JFM and SOI JFM accurately classified JFM precipitation as above or below normal for 17 out of 21 years, corresponding to a KSS of 61.91. This was confirmed with an equal KSS through CV. There were no significant JAS predictors in any period. Similarly, in looking at JFM streamflow, there was only one combination during one period of the study that was significant in LDA. Together, AMO OND, AMO JFM, and PNA JFM achieved a KSS of 71.43 (18:21 years correctly classified) during the positive PDO years, and this was confirmed with CV at a slightly lower KSS of 61.91 (17:21). These relationships are of little predictive value.

In separate runs using wintertime averages and JAS averages as predictors for JFM snowfall, significant results occurred for each, but during different periods of the study. During the negative PDO years, EN34 JFM, SOI JFM, and NAO JFM achieved a KSS of 75.0 (28:32) in determining JFM snowfall with LDA. This was confirmed with a CV skill score of 62.5 (26:32). A truly predictive equation for streamflow uses JAS averages as predictors, the combination of AMO, PDO, and PNA. It achieved a KSS of 80.95 (19:21) with LDA during the positive PDO years. The CV KSS of 52.38 corresponds to 16 out of 21 years being correctly classified in above or below normal bins.

Directly using atmospheric/oceanic oscillation indices (and the preceding October reservoir level) as predictors of May reservoir levels, the single best predictor in all time periods was the previous October reservoir level. In this case the highest KSS values are relatively low, the highest was 43.71 (23:32 correct) during negative PDO years. The only highly significant combination of predictors for the peak reservoir levels was found to be PNA JFM and October reservoir levels, and only during negative PDO years. The LDA KSS for this combination was 68.75 (27:32), and this value was also achieved with CV. There were no other significant results.

Finally, in using hydrological parameters as predictors for May reservoir levels, significant results were only found in the negative PDO period. Using three variables during the negative period, streamflow O-A, snowfall JFM, and precipitation JFM achieve a KSS of 81.25 (29:32) during LDA. This combination of discriminators gave a KSS of only 56.25 (25:32) with CV.

As the above LDA and CV results demonstrate, it may be possible to accurately predict hydrological factors and annual peak reservoir levels within the NYC watershed. However, at this point these results offer little in terms of practical applications. Using JFM averages, for example, as predictors may be interesting, but they do not provide enough lead time to plan resource management. Combinations of predictors from antecedent periods offer little in terms of predictive capability. For long-term resource management purposes this study may provide a good starting point for additional research. The ability to either empirically, or physically, predict NAO, PDO, etc. phase with lead times of at least a season, will provide a means of applying these empirical results to water management decisions in the NYC watershed. Additional research to more fully understand the mechanisms that drive these empirical findings will also increase the potential of seasonal hydrologic forecasts in the Northeast.

APPENDIX A

Oscillation Definitions

Atlantic Multidecadal Oscillation (AMO): A basin-wide, 60-80 year cycle of sea surface temperature anomalies in the Atlantic Ocean north of the equator. The index is modified to remove the impact of the El Niño-Southern Oscillation cycle. Anomalies range +/- 0.4°C (Enfield, et al. 2001). Warm phases have occurred 1860-80 and 1940-60 and cool phases 1905-25 and 1970-90. Initially named by Kerr (2000).

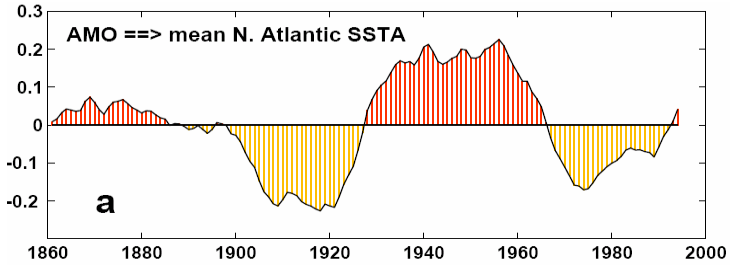

Figure 12: The AMO cycle, 1860-1995. From Enfield, et al. (2001)

El Nino-Southern Oscillation (ENSO): Under normal conditions in the equatorial Pacific Ocean, strong easterly trade winds pile warm water along Australia and southeastern Asia. When the eastern trade winds subside, the pooling of warm water occurs farther east along the equator in the region of 5°S to 5°N, 90°W-160°E. This part of the cycle is referred to as El Niño. La Niña is the strengthening of the trades (to greater than normal) and subsequent cold upwelling that follows in the same region. The El Niño index used here is a three-month average of SSTAs (as derived from the 1971-2000 normals). If, for three months, the SSTA in the Niño 3.4 region (5°S-5°N, 120°W-170°W) is consecutively greater than (less than) 0.5°C, an El Niño (La Niña) phase is considered to be occurring. The Southern Oscillation is the atmospheric component of ENSO. Lower pressure develops over the

more eastern pool of warm water in El Niño due to rising heat/air, while near Australia cooler than normal SSTs favor high pressure development. ENSO episodes typically last 9-12 months. (http://www.cpc.ncep.noaa.gov/products/analysis_monitoring/ensostuff/ensofaq.html#NINO,http://www.nws.noaa.gov/ost/climate/STIP/ElNinoDef.htm).

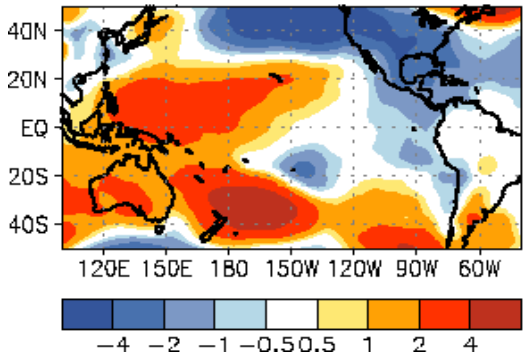

Figure 13a: SSTAs during El Niño (°C)

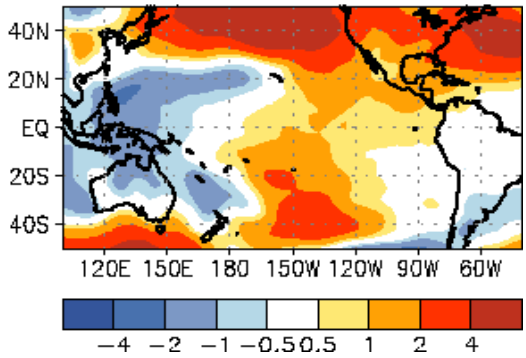

Figure 13b: SSTAs during La Niña (°C)

(Figures 13a and 13b from http://www.cpc.ncep.noaa.gov/products/analysis_monitoring/ensocycle/ensocycle.html)

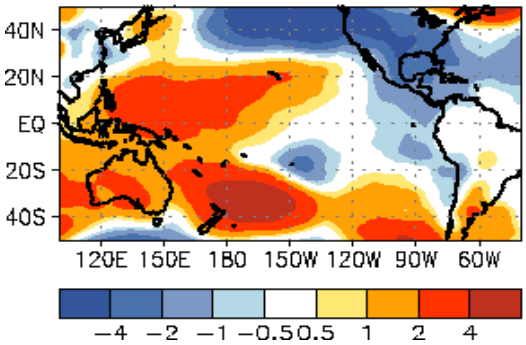

Figure 13c: SLP anomalies during El Niño (hPa)

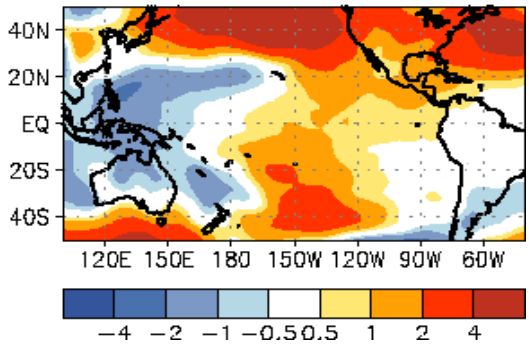

Figure 13d: SLP anomalies during La Niña (hPa)

(Figures 13c and 13d from http://www.cpc.ncep.noaa.gov/products/analysis_monitoring/ensocycle/soilink.html)

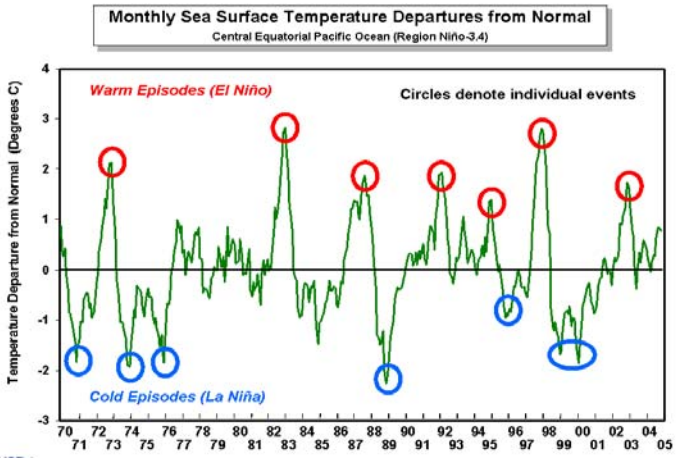

Figure 14: SSTAs for Equatorial Pacific. (Image from http://www.usda.gov/oce/waob/jawf/enso/sstdep.gif)

North Atlantic Oscillation (NAO): A "seesaw" in effect between the Azores high pressure and Icelandic low pressure. It is considered to be in a positive phase when the low is deeper than normal and the high is stronger than normal. The positive phase is associated with more frequent and stronger winter storms crossing the Atlantic Ocean on a more northerly route. A negative phase is considered to be in place when the SLP anomalies are very mild. The weaker cross-Atlantic winter storm track is associated with cold air dipping farther south in the eastern United States. The NAO index itself is a measurement of the SLP difference between the Azores high and the Iceland low pressures (http://www.ldeo.columbia.edu/NAO).

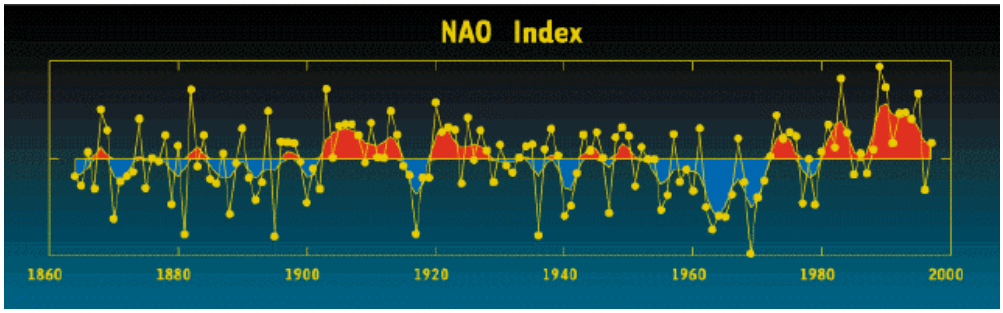

Figure 15a: NAO Index, 1863-1998. (Image from http://www.ldeo.columbia.edu/NAO/)

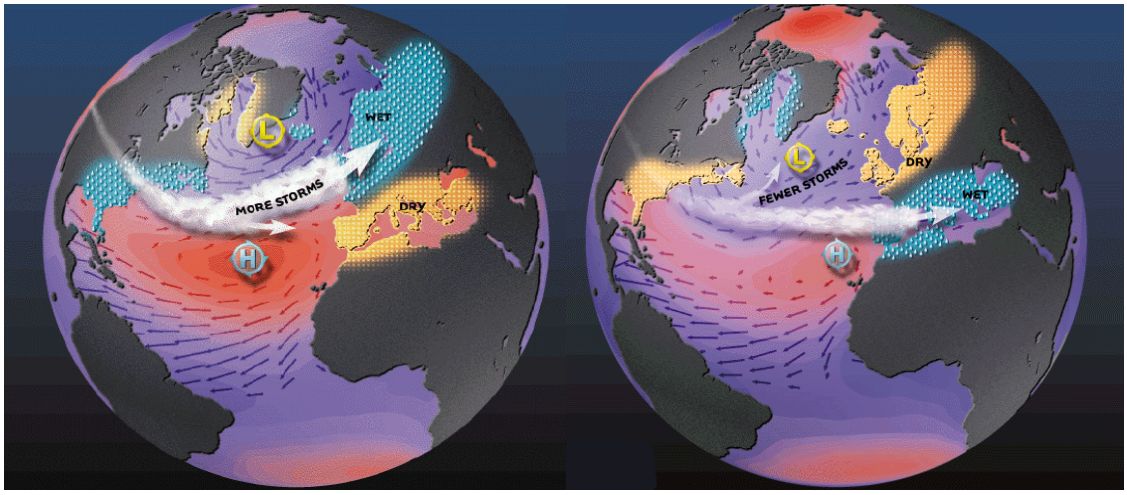

Figure 15b: Positive NAO general scenario

Figure 15c:Negative NAO general scenario

(Figures 15b and 15c from http://www.ldeo.columbia.edu/NAO/)

Pacific Decadal Oscillation (PDO): A pattern of SSTAs in the Pacific Ocean similar to El Niño, but with a periodicity of 20-30 years and weaker anomalies. A positive (negative) PDO phase is marked by a warmer-(cooler) than-normal equatorial region and eastern basin with the North Pacific being cooler (warmer) -than-normal. The PDO index itself is "the leading PC from an un-rotated empirical orthogonal function (EOF) analysis of monthly residual North Pacific SSTAs" north of 20°N, with residuals being defined as "the difference between observed anomalies and the monthly mean global average SSTA" (Mantua and Hare, 2002).

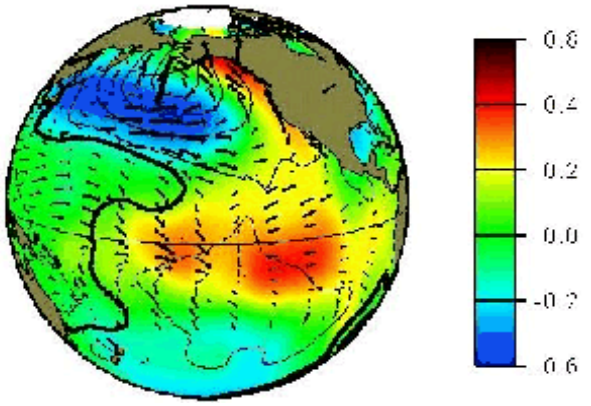

Figure 16: SSTAs associated with +PDO phase. (Image courtesy of http://tao.atmos.washington.edu/pdo/img/pdo_enso_comp.gif)

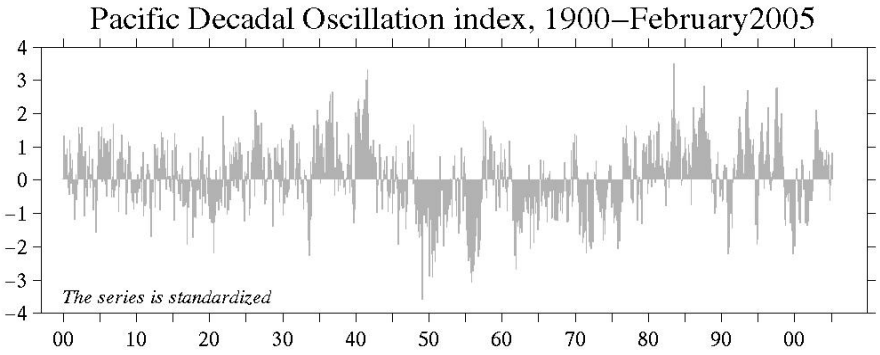

Figure 17: PDO standardized time series (Image courtesy of http://www.jisao.washington.edu/data_sets/pdo/pdo.jpg)

Pacific-North American Oscillation (PNA): Is defined as the second leading mode of rotated principal component analysis (RPCA) of the monthly average 500 hPa height for 1950-2000. It is one of "the most prominent modes of low-frequency variability in the Northern Hemisphere extratropics, appearing in all months except June and July," according to NOAA's Climate Prediction Center (http://www.cpc.ncep.noaa.gov). PNA presents itself as a "quadripole"

of height anomalies over North America with Hawaii and central Canada experiencing anomalies opposite to those over Alaska and the southeastern United States. On average, a dominant PNA phase (positive or negative) remains in place for 2+ years. A positive (negative) PNA is associated with more meridional (zonal) flow over the United States, bringing a more (less) active weather pattern.

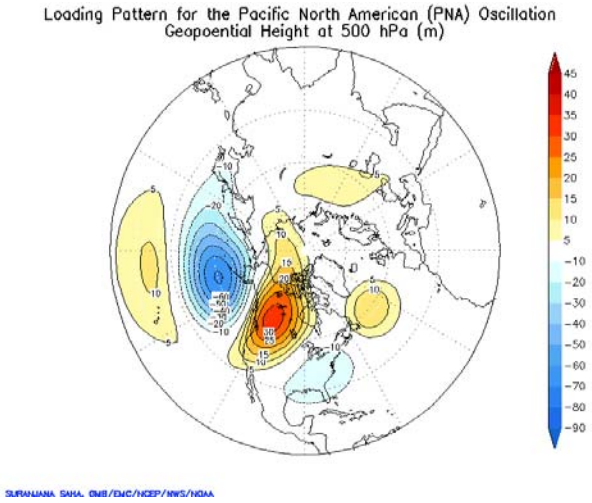

Figure 18: Height anomalies associated with PNA at 500 hPa. (Image from http://www.emc.ncep.noaa.gov/gmb/ssaha/indices/pna_load.gif)

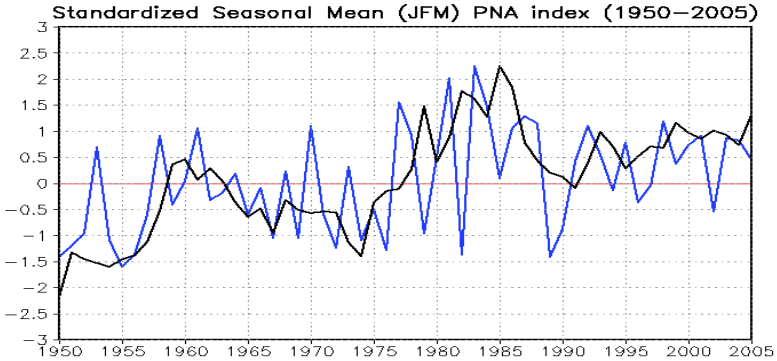

Figure 19: PNA JFM average, 1950-2005. (Image from http://www.cpc.ncep.noaa.gov/products/precip/CWlink/pna/season.JFM.pna.gif)

APPENDIX B

```
A=[0, .35, .52, .754, -.55]
B=[1.2, 3.6, 0.7, 2.2, 4.8]
placeholders=[0,1,2,3,4]
PDO = [0,0,1,1,0]
import random
import stats

def arrange_series(series):
    rearranged_series = [‘’,]*len(series)
    for count in range(len(series)):
        index = placeholders[count]
        rearranged_series[count] = series[index]
    return rearranged_series

for num in range(10000):
    rand_Aneg = []
    rand_Apos = []
    rand_Bneg = []
    rand_Bpos = []
    random.shuffle(placeholders)
    rand_A = arrange_series(A)
    rand_B = arrange_series(B)
    for years in range (len(PDO)):
        if PDO[years] == 0:
            rand_Aneg.append(rand_A[years])
            rand_Bneg.append(rand_B[years])
        if PDO[years] == 1:
            rand_Apos.append(rand_A[years])
            rand_Bpos.append(rand_B[years])

    (corrNEG,probNEG) =stats.lpearsonr(rand_Aneg, rand_Bneg)
    (corrPOS,probPOS) =stats.lpearsonr(rand_Apos, rand_Bpos)
    if corrPOS-corrNEG > 0.57:
        print “Correlation During (-) PDO/(+) PDO:”, corrNEG, “/”, corrPOS
```

A, B: Time series being correlated

Placeholders: shuffled so that series A and B are still paired correctly

PDO: 0=negative, 1=positive

Python modules imported to define reshuffling and statistical functions

Defining the series to be shuffled (the placeholders) and tying the placeholders to the time series

Instructions to run test 10,000 times

Creating empty series to hold newly rearranged A and B series, divided into +PDO and -PDO

Shuffle placeholders

Define rand_A and rand_B as the A and B series rearranged like the shuffled placeholders

Split up newly arranged time series into +PDO and –PDO years

Print correlation results if their difference between phases is greater than a specified value

Correlate time series separately for +PDO and –PDO years

REFERENCES

Bradbury, J.A., B.D. Keim, and C.P. Wake. 2003. The influence of regional storm tracking and teleconnections on winter precipitation in the northeastern United States. *Annals of the Association of American Geographers*, 93:3, 544-556.

Cayan, D.R. and D.H. Peterson. 1989. The influence of North Pacific atmospheric circulation on streamflow in the West. In *Aspects of Climate Variability in the Pacific and Western Americas*, D.H. Peterson, ed., Geophys. Monogr. 55. Washington, DC: American Geophysical Union.

DeGaetano, A.T. 1999. A temporal comparison of drought impacts and responses in the New York City Metropolitan Area. *Climatic Change*, 42: 539-560.

DeGaetano, A.T., M.E. Hirsch, and S.J. Colucci. 2002. Statistical prediction of seasonal east coast winter storm frequency. *Journal of Climate*, 15:10, 1101-1117.

Dettinger, M.D., D.R. Cayan, G.J. McCabe, and J.A. Marengo. 2000. Multiscale streamflow variability associated with El Niño/Southern Oscillation. In *El Niño and the Southern Oscillation: Multiscale Variability and Global and Regional Impacts*. Ed. H.F. Diaz and V. Markgraf. Cambridge, U.K.: Cambridge University Press.

Dracup, J.A. and E. Kahya. 1994. The relationships between U.S. streamflow and La Niña events. *Water Resources Research*, 30:7, 2133-2141.

Enfield, D.B. and A.M. Mestas-Nuñez. 2001. Interannual to Multidecadal climate variability and its relationship to global sea surface temperatures. In *Interhemispheric Climate Linkages*. Ed. V. Markgraf. San Diego, CA: Academic Press.

Enfield, D.B., A.M. Mestas-Nuñez, and P.J. Trimble. 2001. The Atlantic Multidecadal Oscillation and its relation to rainfall and river flows in the continental U.S. *Geophysical Research Letters*, 28:10, 2077-2080.

Gershunov, A., and T.P. Barnett. 1998. Interdecadal modulation of ENSO teleconnections. *Bulletin of the American Meteorological Society*, 79:12, 2715-2725.

Gutman, N. B. and Robert G. Quayle, 1996. A historical perspective of U.S. climate divisions. *Bulletin of the American Meteorological Society*, 77:2, 293–303.

Hartley, S. and M.J. Keables. 1998. Synoptic associations of winter climate and snowfall variability in New England, USA, 1950-1992. *International Journal of Climatology*, 18, 281-198.

Hurrell, J.W. 1995. Decadal trends in the North Atlantic Oscillation: regional temperatures and precipitation. *Science*, 269:5224, 676-679.

Kahya, E. and J.A. Dracup. 1993. U.S. streamflow patterns in relation to the El Niño/Southern Oscillation. *Water Resources Research*, 29:8, 2491-2503.

Kerr, R.A. 2000. A North Atlantic climate pacemaker for the centuries. *Science*, 288:5473, 1984-1986.

Latif, M. and T.P. Barnett. 1994. Causes of decadal climate variability over the North Pacific and North America. *Science*, 266:5185, 634-637.

Mantua, N and S.R. Hare. 2002. The Pacific Decadal Oscillation. *Journal of Oceanography*, 58:1, 35-44.

McCabe, G.J., M.A. Palecki, and J.L. Betancourt. 2004. Pacific and Atlantic Ocean influences on Multidecadal drought frequency in the United States. *Proceedings of the National Academy of Sciences of the United States of America (PNAS)*, 101:12, 4136-4141.

Nigam, S., M. Barlow, and E.H. Berbery. 1999. Analysis links Pacific decadal variability to drought and streamflow in the United States. *Eos*, 80:61, 621-25.

Platt, R.H., P.K. Barten, and M.J. Pfefer. 2000. A full, clean glass? Managing New York City's watersheds. *Environment*, 42:5, 8-20.

Rajagopalan, B., E. Cook, U. Lall, and B.K. Ray. 2000. Spatiotemporal variability of ENSO and SST teleconnections to summer drought over the United States during the twentieth century. *Journal of Climate*, 13:24, 4244-4255.

Schwing, F.B., J. Jiang, and R. Mendelssohn. 2003. Coherency of multi-scale abrupt changes between the NAO, NPI, and PDO. *Geophysical Research Letters*, 30:7, 1406-1409.

Wallace, J.M. and D.S. Gutzler. 1981. Teleconnections in the geopotential height field during the Northern Hemisphere winter. *Monthly Weather Review*, 109, 784-812.

Wang, H. and R. Fu. 2000. Winter monthly atmospheric anomalies over the North Pacific and North America associated with El Niño SSTs. *Journal of Climate*, 13:19, 3435-3447.

Wilks, D.S. 1995. *Statistical Methods in the Atmospheric Sciences: An Introduction*. San Diego, CA: Academic Press.